Acta Chemica Scandinavica A 28 (1974) 61—70

Magnetic Structures and Properties of $Mn_{1-t}Fe_tAs$ Phases

KARI SELTE, [a] ARNE KJEKSHUS [a] and ARNE F. ANDRESEN [b]

[a] Kjemisk Institutt, Universitetet i Oslo, Blindern, Oslo 3, Norway and [b] Institutt for Atomenergi, Kjeller, Norway

The pseudo-binary MnAs-FeAs system has been investigated by X-ray and neutron diffraction, density, magnetic susceptibility, and magnetization measurements. $Mn_{1-t}Fe_tAs$ exhibits temperature dependent regions of limited solid solubility with a virtually constant 1:1 ratio between the metal and non-metal components. The crystal structure is of the MnP type at room temperature, except for a very small range near the composition MnAs where the NiAs type structure prevails.

In the range $0.00 \leqq t < \sim 0.12$, high temperature X-ray and neutron diffraction and magnetic susceptibility measurements demonstrate a transition from MnP to NiAs type structure at temperatures between 385 and 575 K, depending on composition. The temperature dependence of the magnetic susceptibility obeys the Curie-Weiss Law in the region of the NiAs type structure (*viz.* the high temperature phase for $t \approx 0$) with an essentially constant (paramagnetic) spin quantum number of $2S_T = 3.7 \pm 0.2$ ("spin only" approximation) per metal atom. The low temperature phase with NiAs type structure is found to exhibit ferromagnetism in agreement with previous studies. In the region of the MnP type crystal structure, a helimagnetic ordering of the spins is adopted at low temperatures ($T_N = 206 \pm 1$ K for $t = 0.10$) with spiral propagation along the a axis ($0.133 \times 2\pi\mathbf{a}^*$ for $t = 0.10$ at 90 K; the setting of the MnP type unit cell is in accordance with space group *Pnma*). The magnetic structure is of the double spiral type previously found for compounds with the MnP type structure, but differs by propagating along the a axis and by having a different phase relation between the spirals. The spiral periodicity is rather temperature dependent.

No crystallographic transformations have been observed between 4.2 and 1300 K within the interval $\sim 0.65 < t \leqq 1.00$, where the reciprocal magnetic susceptibility cannot be expressed as a simple linear function over an appreciable temperature range, implying that the Curie-Weiss Law is not satisfied. An antiferromagnetic structure with doubling of the crystallographic a and c axes is found in the composition range $0.65 \leqq t < \sim 0.90$ at lower temperatures ($T_N = 54 \pm 1$ K for $t = 0.85$ where, moreover, $\mu_T (= 2S_T) = 0.71 \pm 0.04$ μ_B at 13.5 K). A double helix magnetic spin arrangement along the c axis is adopted in a narrow region close to FeAs.

The endeavour within many research fields has a tendency to oscillate, for various reasons, between periods of low and high activity. This is rather characteristic of the historical development of the investigations on phases with the MnP type crystal structure. An initial diligent period primarily devoted to syntheses, phase analyses, and approximate structure determinations was followed by one of less attention, which in turn was relieved in 1966 by a more intense period with the emphasis centered mainly on magnetic properties. It is clearly impossible, at this stage, to estimate the significance of the achievements in the latter, hitherto incomplete, period. However, the binary MnP phases have apparently been fully explored by the experimental methods available at present without providing a credible clue as to their strange magnetic behaviour. Faced with this unsatisfactory situation it is natural to turn to the ternary MnP phases. The MnAs-FeAs system was selected as the first target for the extension of our research programme.

EXPERIMENTAL

Samples of MnAs and FeAs were made by heating weighed quantities of the elements [99.9+ % Mn (The British Drug Houses; crushed powder from the commercial, electrolytic grade material), 99.99+ % Fe (Johnson, Matthey & Co.; turnings from rods), and 99.9999 % As (Koch-Light Laboratories)] in

evacuated, sealed quartz tubes. FeAs was prepared as described in Ref. 1. During the syntheses of MnAs the temperature was slowly increased to 900°C, the sample was kept at this temperature for 3 days, and then quenched in ice water. After careful grinding, the sample was reheated at 700°C for 10 days and cooled to room temperature over 3 days. The binary arsenides produced in this way were mixed in proportions appropriate to the desired ternary compositions and subjected to a first annealing at 850°C for 8 days. All samples were crushed and subjected to three further annealings at 850°C with intermediate crushings, and finally cooled to room temperature over a period of 3 days or quenched in ice water.

The experimental details concerning the X-ray and neutron diffraction, density, magnetic susceptibility, and magnetization measurements have been presented in previous communications.[1,2]

RESULTS

(i) *Homogeneity ranges and atomic arrangements.* Since the main purpose of the present work is to examine the variation in the magnetic properties of $Mn_{1-t}Fe_tAs$ as a function of t, the necessary phase analysis was minimized to surveying the situation at a single annealing temperature. As a compromise between various competing factors, 850°C was chosen, and in the initial experiments all samples were quenched from this temperature. However, the results unfortunately showed that the quenching technique did not give entirely homogeneous samples, and a slow cooling procedure was accordingly adopted for the subsequent, larger scale syntheses.

The extents of the homogeneity ranges have been determined from the variation of the unit cell dimensions with the composition parameter t (Fig. 1), the overall solubility limits being also confirmed by application of the disappearing phase principle on the X-ray powder data. As evident from Fig. 1, MnAs and FeAs are only partially soluble in each other at temperatures below 850°C. The extent of the Mn rich phase is strongly temperature dependent ($0.00 \leqq t < \sim 0.35$ and $0.00 \leqq t \leqq 0.12 \pm 0.02$ for quenched and slowly cooled samples, respectively) whereas the homogeneity range of the Fe rich phase is essentially temperature independent ($0.65 \pm 0.02 \leqq t \leqq 1.00$).

Apart from $t \approx 0$ all single phase samples exhibit the MnP type crystal structure at room

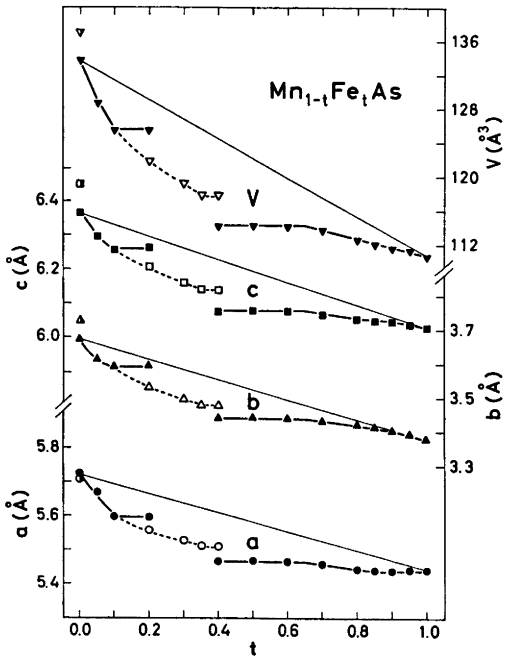

Fig. 1. Unit cell dimensions of the ternary solid solution series MnAs-FeAs as a function of composition. Filled and open symbols represent slowly cooled and quenched samples from 850°C, respectively. Half filled symbols give the corresponding data for the room temperature modification of MnAs with NiAs type structure.

temperature. The pycnometrically determined densities show that the solid solubility is of the strictly substitutional type with a virtually constant 1:1 ratio between the metal and non-metal components. The lack of additional superstructure reflections in the X-ray and neutron diffraction diagrams confirms that the substituted atoms are arranged at random in the metal sublattice.

The positional parameters for the MnP type atomic arrangement vary very little (Table 1) with composition and temperature ($T < 300$ K). (Corresponding data for MnAs and FeAs are given in Refs. 1, 3–5.) This constancy is somewhat remarkable in view of the exceptional position of the MnAs coordinates (at 55°C) in this respect, implying that there must be rather rapid changes in the variables near $t = 0$.

A tentative phase diagram for the pseudo-binary MnAs-FeAs system is presented in Fig. 2. The diagram shows *inter alia* that the Mn rich samples follow the trend from MnAs in that a

Table 1. Unit cell dimensions and positional parameters with standard deviations for some $Mn_{1-t}Fe_tAs$ phases; space group *Pnma*, positions 4(*c*).

t	0.10			0.85			0.95		
T(K)	21	90	293	13.5	81	293	16	81	293
a (Å)	5.537(3)	5.526(3)	5.615(3)	5.442(2)	5.429(2)	5.435(2)	5.450(1)	5.448(1)	5.434(1)
b (Å)	3.483(3)	3.477(3)	3.589(3)	3.372(1)	3.375(1)	3.404(1)	3.344(1)	3.349(1)	3.385(1)
c (Å)	6.151(3)	6.137(3)	6.252(3)	6.034(1)	6.028(1)	6.041(1)	6.031(1)	6.028(1)	6.030(1)
x_T	0.0091(19)	0.0084(21)	0.0126(20)		0.0042(7)	0.0036(7)	0.0041(7)	0.0051(6)	0.0044(5)
z_T	0.2053(25)	0.2101(28)	0.2138(25)	as for	0.1989(5)	0.1997(5)	0.1978(5)	0.1976(4)	0.1988(4)
x_X	0.1967(6)	0.1962(7)	0.2073(6)	81 K	0.1992(7)	0.2006(6)	0.2010(7)	0.2007(6)	0.2007(5)
z_X	0.5805(9)	0.5830(10)	0.5811(11)		0.5766(8)	0.5780(8)	0.5740(10)	0.5753(8)	0.5787(7)

second-order phase transformation from the MnP to the NiAs type structure takes place above room temperature, the transformation temperature *versus* concentration relationship being approximately linear. For the purpose of comparison, Fig. 2 includes data for the CrAs-MnAs system,[6] where a similar phase relationship is observed.

(ii) *Magnetic susceptibility and magnetization.* The gradual change in the temperature dependence of the magnetic susceptibility with progressively increasing concentration of Fe is shown in Fig. 3.

In the Fe rich phase all characteristics show a consistent change from being convex towards the temperature axis at the lowest temperature to concave at higher temperatures. For FeAs the $\chi^{-1}(T)$ curve has a linear range between ~ 300 and ~ 650 K, which permits a deduction of a tentative value for its paramagnetic moment.[1] Already in the $\chi^{-1}(T)$ curve for $t = 0.95$, this linear dependence is completely destroyed and, in fact, none of the samples within the composition range $0.65 \leqq t < 1.00$ satisfied the Curie-Weiss Law. Hence, information concerning the number of unpaired electrons in the paramagnetic state of the Fe rich phase is inaccessible. The magnetic susceptibility of the samples with $0.65 \leqq t < 1.00$ has not been examined below 80 K, and for this reason the

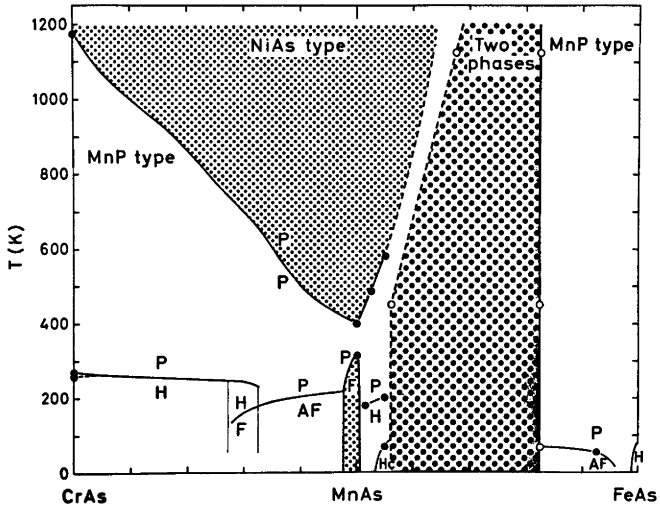

Fig. 2. Diagram of phase relations in the pseudo-binary CrAs-MnAs and MnAs-FeAs systems. Data for the CrAs-MnAs system are quoted from Kazama and Watanabe.[6] Phase boundaries indicated by broken lines are uncertain. The location of the open circles along the temperature axis should be regarded as somewhat undetermined. Magnetic state is indicated by: AF antiferro., F ferro., H helical, P para., c conical.

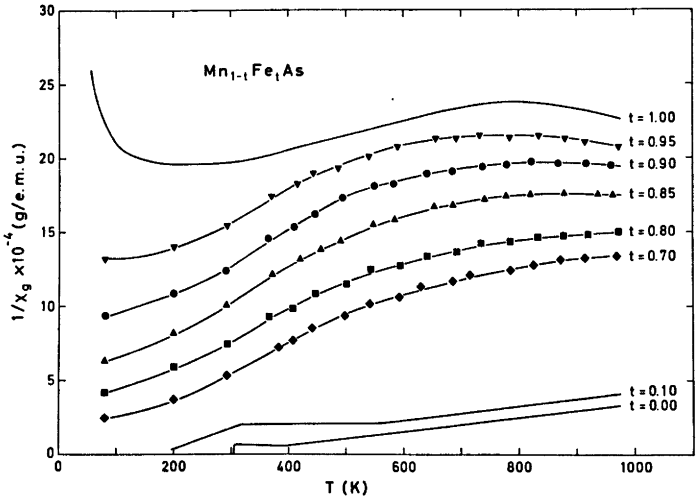

Fig. 3. Reciprocal magnetic susceptibility *versus* temperature for typical $Mn_{1-t}Fe_tAs$ samples.

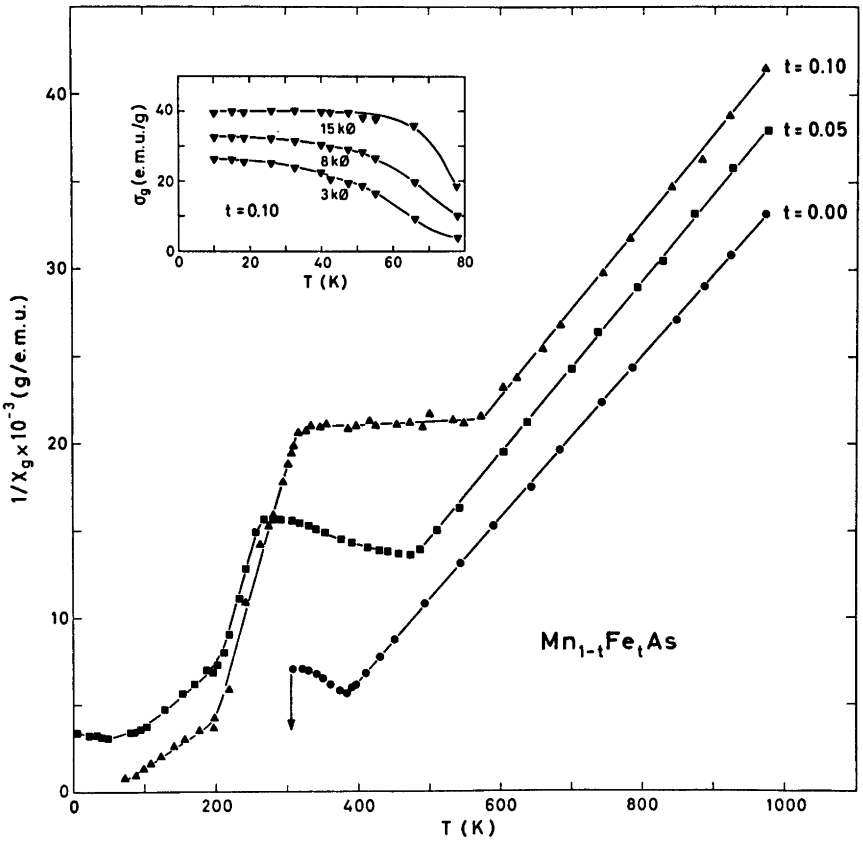

Fig. 4. Thermomagnetic data for Mn-rich $Mn_{1-t}Fe_tAs$ samples.

possible completion of a convex portion of the $\chi^{-1}(T)$ curves towards a rapid increase at lower temperatures could not be verified (*cf.* Fig. 3).

The physical origin of the anomalous $\chi^{-1}(T)$ curves for the Fe rich phase is essentially unknown. Variation in the electronic band structure with temperature may, in principle, account for the observations, but such an explanation must be subject to a future experimental and/or theoretical verification.

The magnetic behaviour of the Mn rich phase is shown in more detail in Fig. 4. These data are more in line with the requirements of conventional theories of magnetism. The present data for MnAs (Fig. 4), which are in excellent agreement with those reported earlier (*cf.*, *e.g.*, surveys in Refs. 7, 8), concur with those for the samples $t=0.05$ and $t=0.10$.

As shown in Fig. 4, the three samples obey almost perfectly the Curie-Weiss Law at high temperatures. The linear $\chi^{-1}(T)$ curves are interrupted at temperatures which correspond very closely to the values obtained, by other means, for the transformation from the NiAs to the MnP type structure. The paramagnetic moment derived according to the "spin only" formula from the high temperature paramagnetic portions of the $\chi^{-1}(T)$ curves, corresponds to an essentially constant spin quantum number of $2S_T=3.7\pm0.2$ per metal atom.

The virtually horizontal, intermediate portions of the $\chi^{-1}(T)$ curves are, according to the neutron diffraction data, to be associated with the paramagnetic state of the MnP type structure of the phase. The temperature dependence of $\chi^{-1}(T)$ within these intervals can again, in principle, be accounted for by assuming gradual changes in the electronic band structures. In this case, there is also experimental evidence available which favours this interpretation (*vide infra*).

On the low temperature side the three curves in Fig. 4 have in common a rapid fall in χ^{-1}. The differences between the three curves at the lower temperatures, which are also clearly demonstrated in the magnetization data (see inset), are due to distinctions in magnetic structure. In accordance with previous findings and the magnetic structure, the magnetization of MnAs is very strong. No detectable zero field magnetization has been observed for the sample with $t=0.05$, whereas the sample with $t=0.10$ exhibits magnetization of intermediate strength (*vide infra*).

The information derived from the magnetic susceptibility data is incorporated in the phase diagram in Fig. 2.

(iii) *Magnetic structures.* The helimagnetic arrangement in pure FeAs extends slightly into the ternary range. According to the results obtained for the sample with $t=0.95$ a tentative boundary is indicated in the phase diagram (Fig. 2) as $t=\sim0.98$. The parameters specifying the spirals are $T_N=77\pm1$ K, $\mu_T=0.5\pm0.1$ μ_B, $\tau=0.375\times2\pi c^*$ for FeAs at 12 K.[1] The helimagnetic structure of FeAs is illustrated in Fig. 5A.

In the range $0.65\leqq t<\sim0.90$ an antiferromagnetic spin structure with doubled a and c axes relative to the chemical unit cell prevails. The Néel temperature varies comparatively little with composition, and is 54 ± 1 K for $t=0.85$. The normalized intensity of the magnetic reflection 101 *versus* reduced temperature for $t=0.85$ follows closely the Brillouin function for $2S=1$. The antiferromagnetic structure is maintained down to liquid helium temperature.

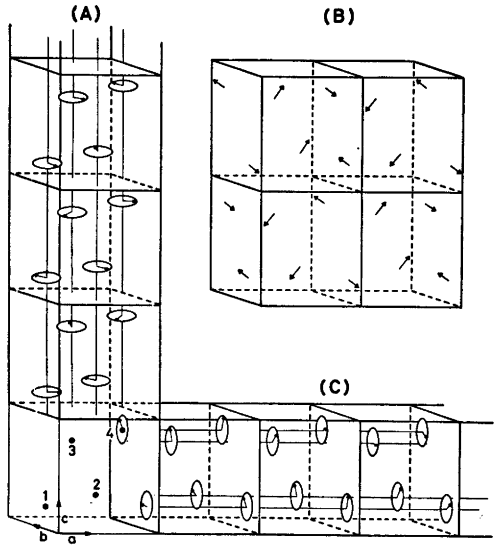

Fig. 5. Spin arrangements in $Mn_{1-t}Fe_tAs$ phases: (A) helical arrangement in FeAs (12 K), (B) antiferromagnetic arrangement in $Mn_{0.15}Fe_{0.85}As$ (13.5 K), and (C) helical arrangement in $Mn_{0.90}Fe_{0.10}As$ (90 K).

Unfortunately the neutron diffraction diagrams contain only a few, rather weak magnetic reflections. Hence, it is impossible to establish the magnetic arrangement unambiguously, and the proposed magnetic structure for $Mn_{0.15}Fe_{0.85}As$ shown in Fig. 5B should only be regarded as a chemically and physically reasonable model which can be adjusted to the observed neutron diffraction pattern at 13.5 K. The model depicted in Fig. 5B consists of two interpenetrating, mutually perpendicular spin systems within (100), the spin of (say) metal atom No. 1 making an angle of $\sim 30°$ with the b axis. (To facilitate comparison between the spin arrangements in Fig. 5B and C, the former may also be regarded as consisting of spirals propagating along the a axis with a periodicity equal to two unit cell lengths.) The value of $\mu_T = 0.71 \pm 0.04$ μ_B derived through the least squares refinement process is consistent with the temperature dependence of the 101 reflection (*vide supra*). On going from $t = 0.85$ to $t = 0.65$ only minor variations are observed in the intensities of the magnetic reflections. This demonstrates that the cooperative magnetic parameters are essentially invariable over the composition interval.

Apart from a narrow region near $t = 0$, where the NiAs type atomic arrangement gives rise to a ferromagnetic state, the Mn rich phase ($\sim 0.01 < t < \sim 0.12$) obtains a helimagnetic ordering below a Néel temperature which varies between 180 ± 3 K for $t = 0.03$ and 206 ± 1 K for $t = 0.10$. The helical arrangement is in this case directed along the a axis (contrary to what has been found hitherto for compounds with MnP type structure; *cf.* Ref. 1) with an overall propagation vector of $0.133 \times 2\pi\mathbf{a}^*$ for $t = 0.10$ at 90 K. The propagation vector is rather temperature dependent between 90 K and T_N, as illustrated in the upper part of Fig. 6 where the spiral turn angle (α) is plotted against temperature. Further parameters specifying the spiral structure are obtained from the abcences ($hk0$ with $h = 2n+1$ extinguished) governing the satellite reflections, and the intensities of those present. In terms of the labelling of the four equivalent metal positions in the unit cell shown on Fig. 5 (*cf.* Refs. 1, 2) these extinctions imply that the spins on atoms 1 and 2 (and equivalently on 3 and 4) are in phase. (It should be noted that for the double c axis spirals previously found atoms 1 and 3, and 2 and 4 are in phase; *cf.* Fig. 5A for the case of FeAs.[1]) By assuming that the magnetic moments μ_T are at right angle to the spiral axis (*vide infra*), and of equal magnitude for the independent spirals, there are accordingly two parameters to be determined, *viz.* μ_T and $\phi(=\phi_{1,4})$. A step-wise refinement procedure like that used in earlier work,[1,2] gave $\mu_T = 1.6 \pm 0.1$ μ_B and $\phi = 60 \pm 10°$ for $Mn_{0.90}Fe_{0.10}As$ at 90 K. The spiral arrangement is illustrated in Fig. 5C. It should be emphasized also in this connection that the deductions are based on reflections with, in general, low intensities.

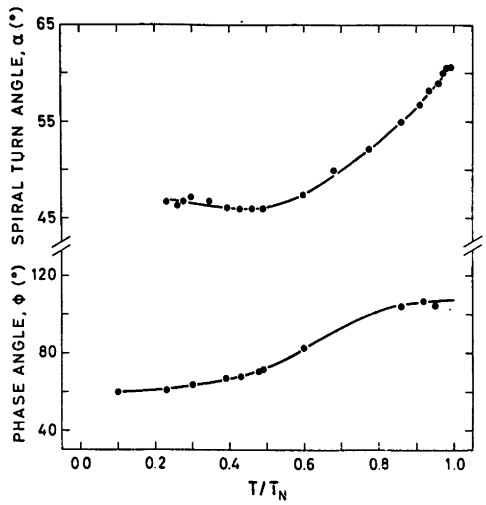

Fig. 6. Phase and turn angles for the spirals in $Mn_{0.90}Fe_{0.10}As$ as functions of reduced temperature.

The attempts to establish the integrated intensity *versus* reduced temperature relationship for the strongest satellites $000^{\pm}$ and $001^{\pm}$ of $Mn_{0.90}Fe_{0.10}As$ resulted in the somewhat strange looking data shown in Fig. 7. Characteristic features are the drop in intensity at low temperature and the difference in temperature behaviour closer to the Néel temperature. The anomalies in the integrated intensities at low temperatures (< 90 K) correspond rather closely to the onset of field strength dependent magnetic susceptibility in Fig. 4. Comparison of observed and calculated intensities for the whole diagram (21 K; nuclear as well as magnetic reflections) shows that this behaviour can be attributed to a conical deformation of the

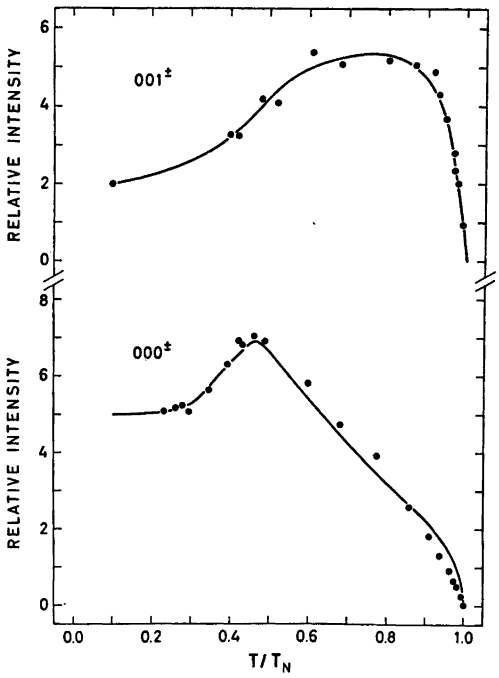

Fig. 7. Temperature dependence of relative integrated intensities of 000± and 001± for $Mn_{0.90}Fe_{0.10}As$.

spiral, the angle between the moments and the spiral axis (β) being estimated to $\sim 60°$. Apart from a slight increase due to the reduction in temperature the total moment remains virtually unaltered. The ferromagnetic component (along the a axis) is 1.0 ± 0.1 μ_B (at 21 K) according to the least squares profile analyses.

Moreover, the marked difference in the temperature variation of the integrated intensities of 000± and 001± (Fig. 7) must be accounted for. The only reasonable explanation of the distinction between the two sets of data for $T/T_N \geqq 0.46$ must be that there is a change in ϕ with temperature. The temperature variation for $T/T_N < 0.46$ is mostly associated with the decreasing cone angle from 90° at $T/T_N = 0.46$ to $\sim 60°$ in the interval $\sim 0.1 < T/T_N < \sim 0.3$. (This effect, which produces the ferromagnetic component in the spiral structure, can be corrected for rather accurately.) Assuming that the apparent reduction in magnetic moment with increasing temperature follows that of FeAs,[1] it is possible to deduce a temperature dependence for ϕ (bottom part of Fig. 6, where it is seen that ϕ increases from 60° at 21 K to 107° at T_N) from the observed intensities of 000± and 001±. As a check of the mutual consistency of the data, the smooth curves in Fig. 7 have been calculated on the basis of the deduced spiral parameters ϕ, β, and μ_T. It is seen that the calculated curves match the experimental points remarkably well. It is worth while to note that the latter agreement also provides additional evidence for the overall correctness of the spiral arrangements in $Mn_{0.90}Fe_{0.10}As$.

In order to observe the position and intensity of 000±, great care had to be taken in improving the collimation and in subtracting the background, which had to be obtained above T_N. The detailed drawing of the peak at the different temperatures revealed the interesting phenomenon shown in Fig. 8. The peak is seen to consist of two partly or completely overlapping reflections, one being considerably stronger than the other. The weaker 000± falls at the high angle side of the stronger at the lowest temperatures ($< \sim 70$ K), whereas the opposite situation prevails at higher temperatures ($> \sim 90$ K). At temperatures where the 000± doublet is partly separated, the intensity of the weaker component has been estimated to 5 – 10 % of that of the main satellite. While the main satellite is shifted only relatively little towards higher angles with increasing temperature, the weaker is shifted more rapidly in the opposite direction.

A similar exploration of the shape of 001± as a function of temperature is more difficult since this reflection is considerably weaker than 000±, but the results indicate a similar behaviour.

The establishment of the doubled 000± and (probably) 001± satellites clearly implies that some of the spiral parameters for $Mn_{0.90}Fe_{0.10}As$ given above should be corrected. The only reasonable explanation we can find for this doubling of the satellites is that the sample is not quite homogeneous. It is conceivable that the substituted Fe atoms are not uniformly distributed over the metal sublattice and that there are domains of different concentration giving rise to spirals of different periodicities. The amount of the minor component is so small that we cannot detect the other satellites and we are therefore unable to say whether this spiral structure deviates significantly from that

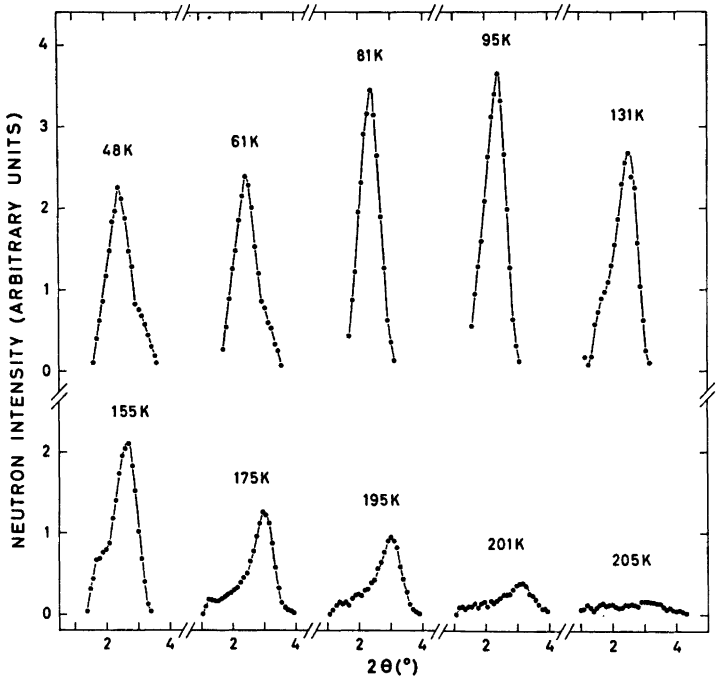

Fig. 8. Profiles of 000± for $Mn_{0.90}Fe_{0.10}As$ at different temperatures; background subtracted.

of the major component. However, since its contribution to the 000± reflection is only 5 – 10 % it can be assumed that very small errors are made by neglecting the inferred correction. It should be emphasized in this connection that in deriving the spiral period and its temperature variation (Fig. 6) for $Mn_{0.90}Fe_{0.10}As$ the peak position of the main 000± satellite has been used, whereas its total intensity has been utilized in obtaining the other spiral parameters (see also Fig. 7).

It should also be remarked that the careful study of the temperature variation of the 000± satellite revealed that this peak does not completely vanish at the Néel point. A small remanent peak is observed several degrees above T_N and moves with increasing temperature to even larger scattering angles. This can be ascribed to a short range spiral order existing above T_N with a periodicity which increases with increasing temperature.

DISCUSSION

The incomplete randomization of Mn and Fe over the metal sublattice may be between the various spiral chains (see Fig. 5C) and/or correspond to local regions of variable t within the chains. Since the spiral period (τ) clearly varies with composition, the occurrence of "concentration domains" would provide a natural explanation, although this raises a number of closely connected questions:

(1) To what degree can an individual, crystallographic character be attributed to the Mn and Fe atoms in a solid solution of this type? Is there a corresponding individuality in their magnetic moments?

(2) Compared with the reflections on X-ray diagrams obtained for a number of other ternary solid solution series of transition metal chalcogenides and pnictides, those of the present Mn rich samples are relatively broad. The corresponding neutron diffraction diagrams are, on the other hand, composed of relatively sharp, nuclear peaks. An explanation of this unexpected result must be sought in the difference in the scattering process, *viz.* in nucleus *versus* electron cloud.

(3) A fundamental problem in connection with (2) is why a substitutionally disordered phase leads to sharp X-ray and/or neutron dif-

fraction diagrams in the general case. An immediate inference of the latter observation is that there is a "constant" average chemical unit cell for each composition which is translated through the crystals. (The metal atoms may well have a degree of individual magnetic character without a corresponding crystallographic identity.)

Closely connected with "concentration domains" is in the present case the occurrence of an insolubility region (Fig. 2). The limited solubility cannot be attributed to a size effect, since the difference in the radius of the metal atom in MnAs [3] and FeAs[1,4,5] is only some 10 %. On the other hand, the distinction in electronic band structure between MnAs and FeAs can, in principle, easily account for the observations. This distinction may either involve the location of the Fermi surface in relation to the Brillouin zone boundaries or be associated with the *d* electron configurations. In connection with the latter suggestion it is of interest to recapitulate that the Mn atoms in the NiAs type structures of MnAs are in "high spin" states, as compared with the "low spin" states generally attributed to the metal atoms in phases with the MnP type structure. No reliable information is unfortunately available for the spin situation in the MnP type modification of MnAs,[9] but this view is supported by the results of magnetic studies of MnAs [10-12] with up to 10 % P substituted for As. The large deviation of the experimental points in Fig. 1 from the linear relationship predicted by Vegard's Law suggests a relatively rapid shrinkage in the size of the Mn atoms near $t=0$. As pointed out in, *e.g.*, Ref. 9 there is a close correlation between atomic size and spin state.

Within the MnAs-FeAs system a wide variety of different types of cooperative magnetism have been found, depending on composition and temperature. Despite distinct difference in formal classification the antiferromagnetic structure within the range $0.65 \leqq t < \sim 0.90$ and the helimagnetic arrangement within $\sim 0.01 < t < \sim 0.12$ are closely related. In both cases the spins are perpendicular to the *a* axis and the crystallographically equivalent metal atoms obtain a corresponding equivalence in the magnetic sense. Similar relations are found when comparisons are made with the cooperative magnetism in $Cr_{1-t}Mn_tAs$ [6] (see also Fig. 2). At the present stage it is impossible to give a more or less complete account for the findings. It is nevertheless tempting to point out some features which appear to be of special interest:

(1) Apart from the region near $t=0$ all the magnetic structures require not less than three exchange parameters to describe their magnetic behaviour.

(2) In the case of MnP, Takeuchi and Motizuki [13] take into account 7 different isotropic (direct and indirect) exchange interactions. Their deductions were based on a number of simplifying assumptions (of which the most important appears to be the assumption $a=b=c$, *i.e.* making the unit cell cubic). Even with the increased translational and internal symmetry of the unit cell, these authors do not provide a complete solution of the exchange interaction problem. Their treatment is limited to prove that the experimental results are consistent with theory. It is feasible that a similar analysis can be performed for the cooperative states of other phases with MnP type structure, but in the lack of a general treatment of the problem such an analysis seems to be of rather limited value.

(3) Similar objections can be raised in connection with Bertaut's [14] treatment of the same problem in terms of two isotropic and one antisymmetric exchange coupling. In fact, the results for FeP,[15] FeAs,[1] $Cr_{1-t}Mn_tAs$,[6] and $Mn_{1-t}Fe_tAs$ suggest very strongly that the number of isotropic and/or antisymmetric exchange couplings must be increased. With such a high number of variables it seems, in principle, possible to account for the observations.

(4) Immediately before this communication was submitted for publication, we received a preprint of a paper by Kallel *et al.*[16] which gives a comprehensive treatment of the exchange interactions in compounds with the MnP type structure. However, as was the case for the treatments by Takeuchi and Motizuki [13] and by Bertaut,[14] the considerations by Kallel *et al.* appear to suffer from a number of weaknesses. In the first place only one of four solutions of the four by four matrix equations is presented in the paper. A more serious objection concerns the fact that only the stability relationship between the ferromagnetic and *c* axis helimagnetic modes are taken into account. Thus, the three antiferromagnetic modes theoretically predicted by Kallel *et al.*, as well as, *e.g.*, the experi-

mentally verified antiferromagnetic and *a* axis helimagnetic modes for $Mn_{1-t}Fe_tAs$ are not considered.

(5) Considering all data for $Mn_{1-t}Fe_tAs$ the magnetic arrangements seem to be determined by details in crystallographic parameters (interatomic distances and angles), electronic band structure (Fermi surface in relation to Brillouin zone boundaries), and the number of unpaired electrons. At present it is tempting to suggest that the behaviour of the itinerant electrons plays an important role in determining the atomic arrangement, and, in particular, the spin orientations.

REFERENCES

1. Selte, K., Kjekshus, A. and Andresen, A. F. *Acta Chem. Scand. 26* (1972) 3101.
2. Selte, K., Kjekshus, A., Jamison, W. E., Andresen, A. F. and Engebretsen, J. E. *Acta Chem. Scand. 25* (1971) 1703.
3. Wilson, R. H. and Kasper, J. S. *Acta Crystallogr. 17* (1964) 95.
4. Selte, K. and Kjekshus, A. *Acta Chem. Scand. 23* (1969) 2047.
5. Selte, K. and Kjekshus, A. *Acta Chem. Scand. 27* (1973) 1448.
6. Kazama, N. and Watanabe, H. *J. Phys. Soc. Japan 30* (1971) 1319.
7. Kjekshus, A. and Pearson, W. B. *Progr. Solid State Chem. 1* (1964) 83.
8. Hulliger, F. *Struct. Bonding (Berlin) 4* (1968) 83.
9. Selte, K. and Kjekshus, A. *Acta Chem. Scand. 25* (1971) 3277.
10. Ido, H. *J. Phys. Soc. Japan 25* (1968) 1543.
11. Hall, E. L., Schwartz, L. H., Felcher, G. P. and Ridgley, D. H. *J. Appl. Phys. 41* (1970) 939.
12. Schwartz, L. H., Hall, E. L. and Felcher, G. P. *J. Appl. Phys. 42* (1971) 1621.
13. Takeuchi, S. and Motizuki, K. *J. Phys. Soc. Japan 24* (1967) 742.
14. Bertaut, E. F. *J. Appl. Phys. 40* (1969) 1592.
15. Felcher, G. P., Smith, F. A., Bellavance, D. and Wold, A. *Phys. Rev. B 3* (1971) 3046.
16. Kallel, A., Boller, H. and Bertaut, E. F. *J. Phys. Chem. Solids. In press.*

Received July 6, 1973.